Smart Rock Technology for Real-time Monitoring of Bridge Scour and Riprap Effectiveness – Design Guidelines and Visualization Tools
(Progress Report No. 6)

Contract No: OASRTRS-14-H-MST
(Missouri University of Science and Technology)

Reporting Period: January 1 – March 31, 2015

PI: Genda Chen

Program Manager: Mr. Caesar Singh

Submission Date: April 15, 2016

TABLE OF CONTENTS

EXECUTIVE SUMMARY

During the sixth quarter of this project, field demonstration tests were carried out at the Gasconade River Bridge (No. A3760), MO. This report summarizes the test results and findings.

I - TECHNICAL STATUS

I.1 ACCOMPLISHMENTS BY MILESTONE

In this quarter, field tests were conducted at the site of US63 Highway Bridge (No. A3760) over the Gasconade River, MO. A smart rock with one N45 magnet in automatically pointing-up system (APUS) was deployed around the upstream side of Bent 4. The test crane was used to facilitate the three-dimensional movement of a 3-axis magnetometer around the deployed smart rock. The 3-axis flux magnetometer sensor head mounted on the test crane was used to measure the magnetic field. A prism mounted on the crane in proximity to the magnetometer sensor was used as a target for coordinate survey by a total station for each measurement point. Finally, the localization of the smart rock was performed based on the magnetic field data and measurement point coordinates.

Task 3.1 Time- and Event-based Field Measurements

In this task, the field tests were carried out on the deck of US63 HWY Gasconade River Bridge as shown in Figure 1. One smart rock was deployed around the upstream side of Bent 4 for bridge scour monitoring. The test crane with a mounted magnetometer sensor was employed to facilitate measurements of the intensity and direction of the magnetic ambient field and the total field after the smart rock had been deployed. Finally, the smart rock SR1 was located from the collected data.

Figure 1 The US63 HWY Gasconade River Bridge

A. Test Setup and Layout

All tests were conducted on the shoulder near the bridge pier at Bent 4 as shown in Figure 2 (a, b). A total station was set near Bent 1 on the Jefferson City side. The center of the total station was used as the origin of a Cartesian coordinate system XYZ with X-, Y-, and Z-axis defined along the transverse, longitudinal (traffic direction), and vertical (upward) directions, respectively. One smart rock, designed by SR1, was deployed at the upstream of Bent 4. The test crane was fixed on a trailer towed by a truck. The magnetometer sensor mounted on the test crane was extended down from the bridge deck to measure the ambient magnetic field and the total magnetic field with the smart rock. Prism 3 mounted below the sensor as shown in Figure 2(c) was used to represent the coordinate of each measurement. Prism 1 and 2 fixed at two ends of the horizontal bar of the test crane were employed to ensure that the horizontal bar was paralleled to the X axis. The measurement points in XOY plane at the location of the sensor were shown in Figure 2(a) at specified Y and Z coordinates near Bent 4. These sensor points were translated to the corresponding forklift locations on the bridge deck, as displayed in Figure 2(d). For each point in XOY plane, seven elevations denoted as Z1, Z2, Z3, Z4, Z5, Z6 and Z7 with equal spacing of 0.3 m were considered for measurements in Z-direction. Therefore, a total of 42 measurement points was taken around Bent 4 in order to locate the SR1 smart rock. The total station set near Bent 1 was used to survey the coordinates (location) of the smart rock and magnetometer sensor as ground true data.

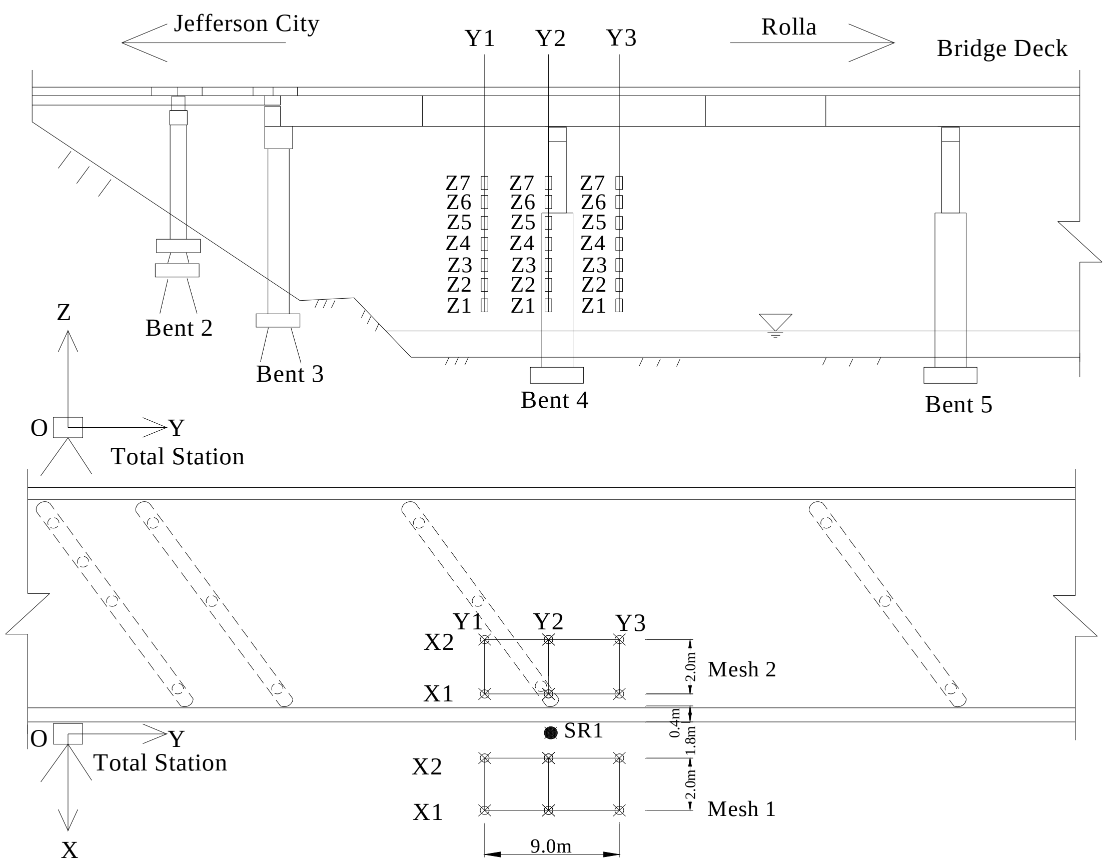

(a) Schematic View of Smart Rock and Sensor Locations in Plane

(b) Layout of Whole Measurement System

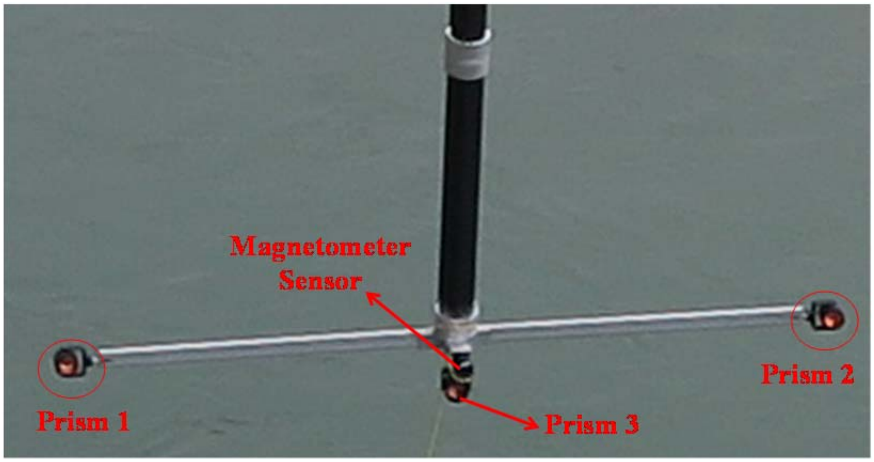

(c) Sensor ang Prisms Positions

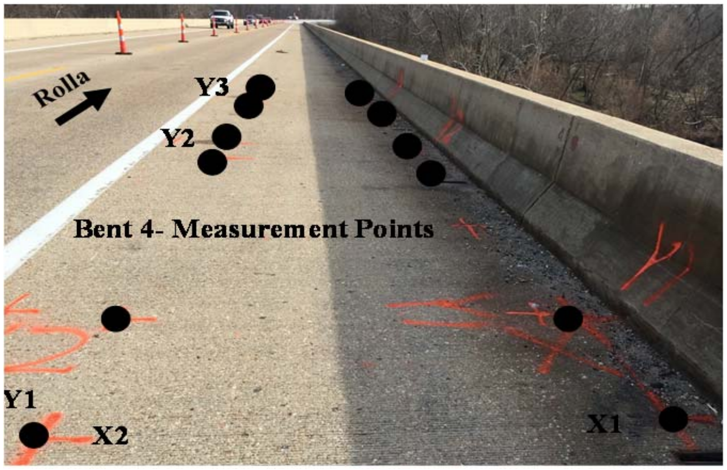

(d) Measurement Points Arrangement

Figure 2 Test Setup at the Site of US63 Gasconade River Bridge

B. Test Procedures

(1) ***Set the XYZ Coordinate System.*** As shown in Figure 3, a proper location for the total station was selected near Bent 1 for its line of sight to the magnetometer sensor, which is designated as Point O or the origin of the coordinate system. The Y-axis point to Rolla was selected to be the longitudinal (traffic) direction of the straight bridge deck, passing through Point O. The X-axis is perpendicular to the Y-axis and pointing to upstream in the horizontal plane, and the Z-axis is upward according to the right hand rule. A permanent point A on the railing of the bridge was also surveyed for future reference.

(2) ***Assemble the Test Crane***. As shown in Figures 2(b), The forklift was first set and tied to an open trailer. The horizontal aluminum arm was then installed and followed by the assemble of ten segments of carbon fiber tubes with 1.0 meter each to lower down the measurement points from the bridge deck. Finally, the horizontal bar was connected at the bottom of the carbon tube to support the magnetometer sensor and prisms for coordinate measurement.

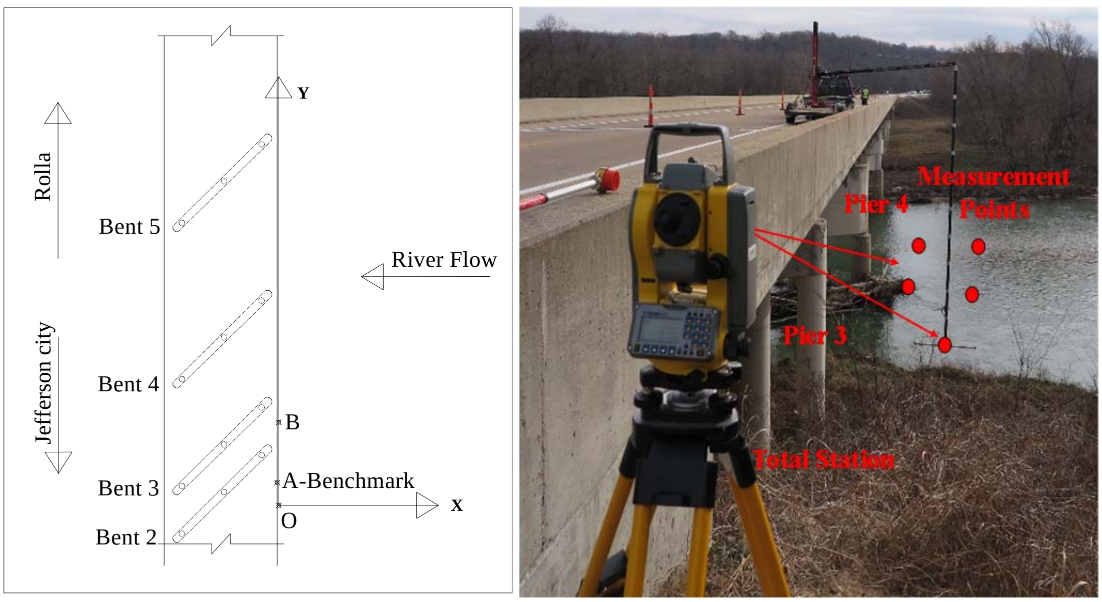

Figure 3 The Coordinate System Selection

(3) ***Set up the STL Digital Magnetometer***. As shown in Figure 2(b), the laptop installed with special software for the sensor controls the measurement of magnetic fields. An Ethernet cable was used to transmit the signal from the sensor to the laptop by an interface called mini Ethernet box. Two batteries were used to power the sensor and laptop.

(4) ***Measure the Ambient Magnetic Field (AMF)***. The ambient magnetic field is generated by the Earth and nearby ferromagnetic objects. It was measured prior to the deployment of the

smart rock. As indicated in Figure 2(a, b, d), the trailer run two paths (X coordinates) on the bridge deck and three stops (Y coordinates). At each stop, seven elevations (Z coordinates) were selected by moving up and down the horizontal beam of the test crane. Figure 4(a) illustrates one stop when by the two rear tires of the trailer are parked at the marked location and the forklift is positioned at Y2X1. At each stop, seven measurements (both coordinate and magnetic field intensity) were taken at seven elevations in Z direction. Therefore, a total of 42 measurements were taken following the entire measurement sequence as indicated in Figure 4(b).

(a) Test Apparatus Located at Y2X2

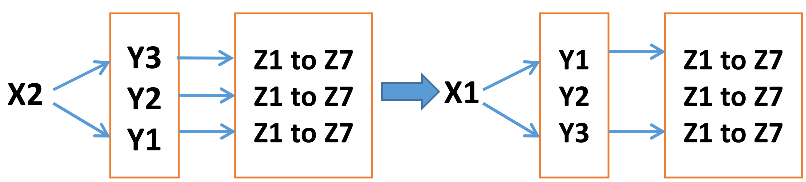

(b) Measurement Point Sequence Arrangement

Figure 4 Arrangement of Ambient Magnetic Field Measurement

(5) ***Deploy the Smart Rock.*** As shown in Figure 5, a smart rock (SR1) with one N45 magnet in APUS configuration described in the previous report was deployed around the upstream of Bent 4 for scour monitoring. The smart rock was tied to a rope and lowered down from the bridge deck to the river bottom at the predetermined site as shown in Figure 6.

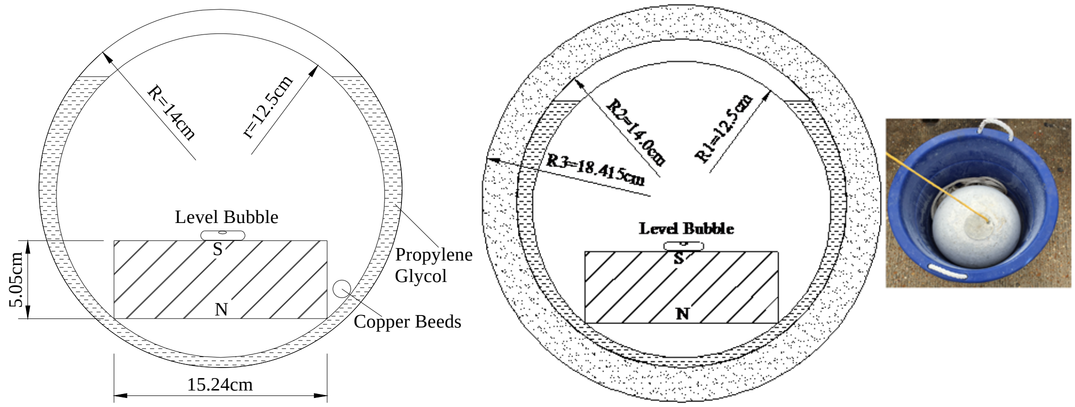

(a) Schematic View (b) Cast Smart Rock

Figure 5 Smart Rock Configuration

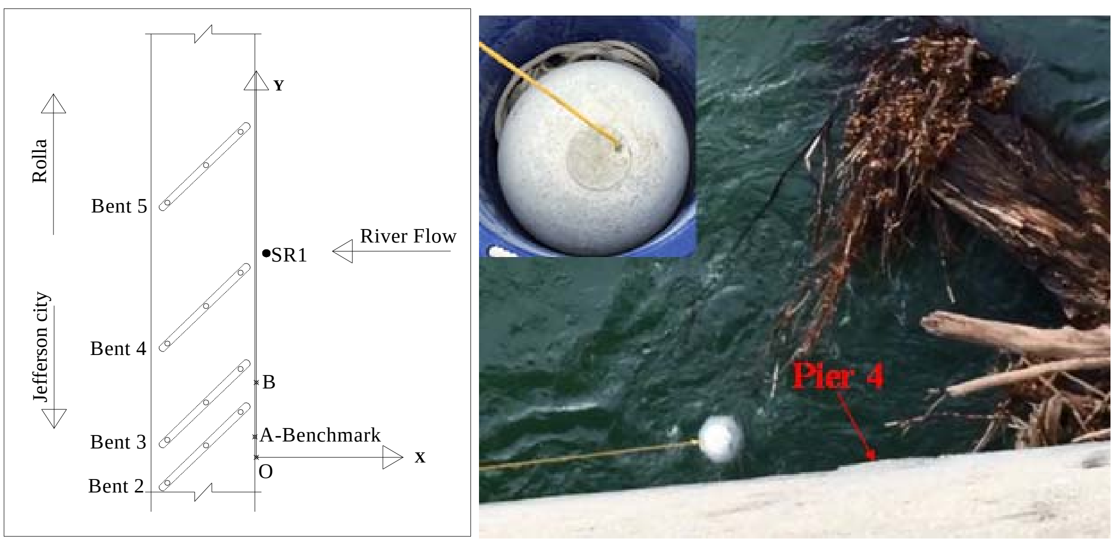

(a) Schematic View of SR1 (b) Deployment of SR1

Figure 6 Deployment of the Smart Rock

(6) ***Measure the Coordinates of the Smart Rock***. The coordinates of the smart rock, SR1, were not measured during the field tests since the water was deep and the water flow was strong so that it was determined to be unsafe to ride a small boat in river and place a prism on the deployed smart rock for measurement. The ground true data will be collected as the water subsides and flow is slow.

(7) ***Measure the Total Magnetic Field***. After the deployment of the smart rock, the total magnetic field combining the effects of the smart rock and the ambient magnetic field was measured following the same procedure as used for the AMF measurement. The total measurement points were also 42 around Pier 4 with the measurement sequence as indicated in Figure 7.

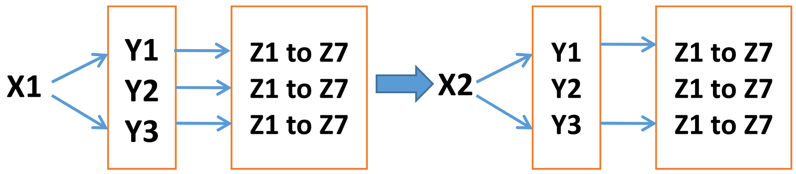

Figure 7 Measurement Sequence for the Total Magnetic Field

D. Localization Algorithm

Eqs. (1) and (2) represent the relationship among the total magnetic field intensity (B), the ambient field (B_{XA}, B_{YA} and B_{ZA}), and the magnetic field of a smart rock at coordinate (X_M, Y_M, Z_M). Both the total and ambient magnetic fields were measured at each measurement point (X,Y, Z). Eq. (3) gives the objective error function that was minimized with respect to the location of the smart rock.

$$B = \sqrt{(B_{XM} + B_{XA})^2 + (B_{YM} + B_{YA})^2 + (B_{ZM} + B_{ZA})^2} \tag{1}$$

$$\begin{pmatrix} B_{XM} \\ B_{YM} \\ B_{ZM} \end{pmatrix} = \begin{pmatrix} -k\dfrac{3(Z-Z_M)(X-X_M)}{\left(\sqrt{(X-X_M)^2+(Y-Y_M)^2+(Z-Z_M)^2}\right)^5} \\ -k\dfrac{3(Z-Z_M)(Y-Y_M)}{\left(\sqrt{(X-X_M)^2+(Y-Y_M)^2+(Z-Z_M)^2}\right)^5} \\ -k\dfrac{2(Z-Z_M)^2-(X-X_M)^2-(Y-Y_M)^2}{\left(\sqrt{(X-X_M)^2+(Y-Y_M)^2+(Z-Z_M)^2}\right)^5} \end{pmatrix} \tag{2}$$

$$J(X_M, Y_M, Z_M) = \sqrt{\sum_{i=1}^{n}[B_i^{(P)} - B_i^{(M)}]^2} \tag{3}$$

E. Test Results and Discussion

Table 1 summarizes the coordinates of 42 measurement points, the AMF intensities prior to deployment of the smart rock, and the total intensities after deployment of the smart rock SR1. The coefficient *k* for the N45 magnet is calculated from the maximum residual flux density. The three components of the total magnetic field (B_x, B_y, B_z) were directly measured by the 3-axis flux magnetometer that was oriented in parallel to the O-XYZ coordinate system. Therefore, the three components of the total magnetic field and the three components (B_{Ax}, B_{Ay} and B_{Az}) of the ambient magnetic field were substituted into the localization algorithm to determine the coordinates of the smart rock SR1.

Table 1 Coordinates and Magnetic Field Intensities at various Measurement Points

		Measurement Points Coordinate (m)			N45 Magnet Factor (nT.m^3)	AMF Intensity (nT)			SR1 & AMF Intensity (nT)
		X_i	**Y_i**	**Z_i**	**K**	**B_{Ax}**	**B_{Ay}**	**B_{Az}**	**B**
Y1X1	Z1	2.931	63.700	-11.014	101770	-16429	-6508	-47393	50756
	Z2	2.918	63.816	-10.680	101770	-16538	-6116	-47364	50686
	Z3	3.071	63.703	-10.388	101770	-16427	-6090	-47349	50664
	Z4	3.072	63.711	-10.072	101770	-16586	-6134	-47224	50579
	Z5	2.942	63.544	-9.832	101770	-16166	-5805	-47357	50491
	Z6	2.944	63.500	-9.482	101770	-16462	-5803	-47184	50468
	Z7	3.016	63.526	-9.198	101770	-16125	-5723	-47231	50370
Y1X2	Z1	2.949	68.191	-10.988	101770	-17208	-7072	-46566	50397
	Z2	2.804	68.282	-10.706	101770	-16981	-7242	-46548	50356
	Z3	2.945	68.164	-10.425	101770	-17261	-7166	-46428	50304
	Z4	2.947	68.195	-10.139	101770	-17356	-7037	-46359	50232
	Z5	2.963	68.186	-9.898	101770	-17287	-7071	-46326	50155
	Z6	2.910	68.101	-9.529	101770	-17271	-6955	-46284	50089
	Z7	2.895	67.757	-9.221	101770	-17613	-6984	-46113	50056
Y2X1	Z1	2.877	72.662	-11.140	101770	-17340	-7834	-46246	50094
	Z2	2.879	72.747	-10.781	101770	-17446	-8167	-46081	50051
	Z3	2.728	72.660	-10.551	101770	-17342	-7765	-46129	49997
	Z4	2.840	72.600	-10.215	101770	-18052	-7498	-45882	49920
	Z5	2.829	72.338	-9.917	101770	-17552	-7699	-45945	49878
	Z6	2.836	72.499	-9.580	101770	-17843	-7691	-45787	49867
	Z7	2.822	72.399	-9.374	101770	-18004	-8253	-45571	49790
Y2X2	Z1	0.828	63.590	-10.965	101770	-16257	-5428	-47393	50597
	Z2	0.806	63.538	-10.629	101770	-16384	-5348	-47302	50547
	Z3	0.807	63.629	-10.366	101770	-16166	-5680	-47269	50490
	Z4	0.854	63.575	-10.076	101770	-16280	-4522	-47348	50415
	Z5	0.850	63.390	-9.810	101770	-16399	-5145	-47144	50389
	Z6	0.844	63.583	-9.435	101770	-16236	-4708	-47178	50288
	Z7	0.843	63.492	-9.131	101770	-15834	-5060	-47160	50171
Y3X1	Z1	0.748	68.182	-10.986	101770	-16445	-7044	-46351	50168
	Z2	0.746	68.082	-10.726	101770	-16876	-7235	-46117	50057
	Z3	0.716	68.060	-10.418	101770	-17230	-6714	-46044	49945
	Z4	0.736	67.896	-10.074	101770	-17212	-6992	-45918	49844
	Z5	0.738	68.085	-9.834	101770	-16834	-6751	-46030	49754
	Z6	0.668	67.994	-9.510	101770	-17037	-6306	-45959	49656
	Z7	0.707	67.749	-9.198	101770	-17072	-6677	-45796	49517
Y3X2	Z1	0.701	72.765	-11.103	101770	-17324	-7543	-45670	49529

	Z2	0.697	72.701	-10.824	101770	-17529	-7748	-45459	49441
	Z3	0.696	72.534	-10.506	101770	-17593	-7944	-45312	49334
	Z4	0.671	72.533	-10.203	101770	-17675	-7779	-45202	49217
	Z5	0.745	72.450	-9.966	101770	-17662	-7494	-45171	49128
	Z6	0.664	72.619	-9.628	101770	-17232	-7765	-45126	49027
	Z7	0.660	72.263	-9.311	101770	-17453	-7916	-44917	48927

Table 2 Predicted and Measured Location of SR1

	X_M/m	Y_M/m	Z_M/m
Predicted SR1 Location	0.460	68.168	-17.002

Table 2 provides the predicted coordinates (X_M, Y_M, Z_M) of the smart rock SR1. It was calculated using the measured coordinate and magnetic intensity at the sensor locations. The predicted location of the smart rock is reasonable based on its relative position to the measurement points.

Task 3.2 Visualization Tools for Rock Location Mapping over Time

Tests to map the profile of the river bed around Bent 4 were delayed since it was not safe to operate a small boat with sonar system installed in strong current.

Task 4 Technology Transfer, Report and Travel Requirements

The 6^{st} quarterly report is being submitted.

I.2 PROBLEMS ENCOUNTERED

In this quarter, the ground true data of the smart rock was not taken due to the strong water current in which it was determined to be unsafe to operate a small boat around the deployed smart rock. Also, the profile mapping of the river bottom around Bent 4 was delayed due to the water condition.

I.3 FUTURE PLAN

The following task and subtasks will be executed during the next quarter.

Task 3.1 Time- and Event-based Field Measurements

The field tests at two bridge sites in Missouri will continue to further validate the localization of smart rocks.

Task 3.2 Visualization Tools for Rock Location Mapping over Time

This task will be actively pursued based on the field test.

Task 4 Technology Transfer, Report and Travel Requirements

The 7^{th} quarterly report will be prepared and submitted.

.

II – BUSINESS STATUS

II.1 HOURS/EFFORT EXPENDED

The planned hours and the actual hours spent on this project are given and compared in Table 3. In the six quarter, the actual hours spent are less than the planned hours, leading to an actual cumulative hour of approximately 121% of the planned hours. The cumulative hours spent on various tasks by personnel are presented in Figure 7.

Table 3 Hours Spent on This Project

	Planned		Actual	
	Labor Hours	Cumulative	Labor Hours	Cumulative
Quarter 1	236	236	176	176
Quarter 2	236	472	294	471
Quarter 3	236	708	294	765
Quarter 4	236	944	523	1288
Quarter 5	236	1180	300	1588
Quarter 6	236	1416	120	1708
Quarter 7	236	1652		
Quarter 8	236	1888		

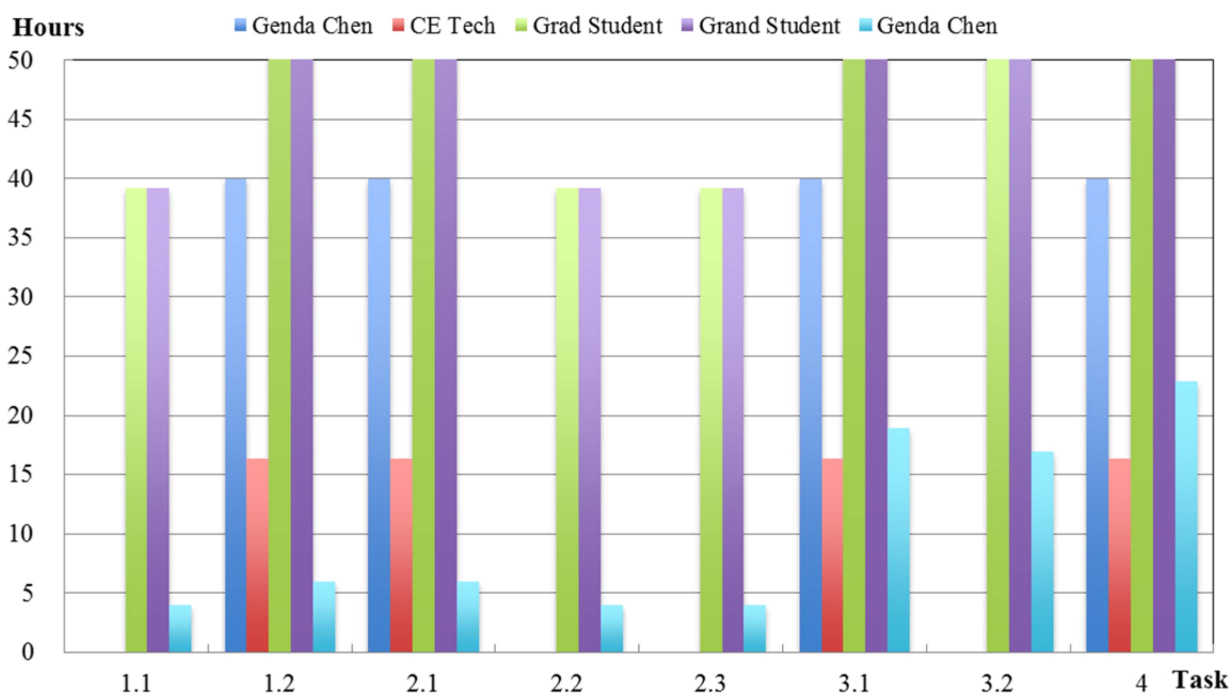

Figure 7 Cummulative Hours Spent on Various Tasks by Personnel

II.2 FUNDS EXPENDED AND COST SHARE

The budgeted and expended OST-R funds accumulated by quarter are compared in Figure 8. Approximately 104% of the proposed budget has been spent till the end of sixth quarter. The actual cumulative expenditures from OST-R, Mo S&T, and MoDOT are compared in Figure 9. The expenditure from OST-R is less than the combined amount from the Mo S&T and MoDOT, meeting the required non-federal match fund requirement.

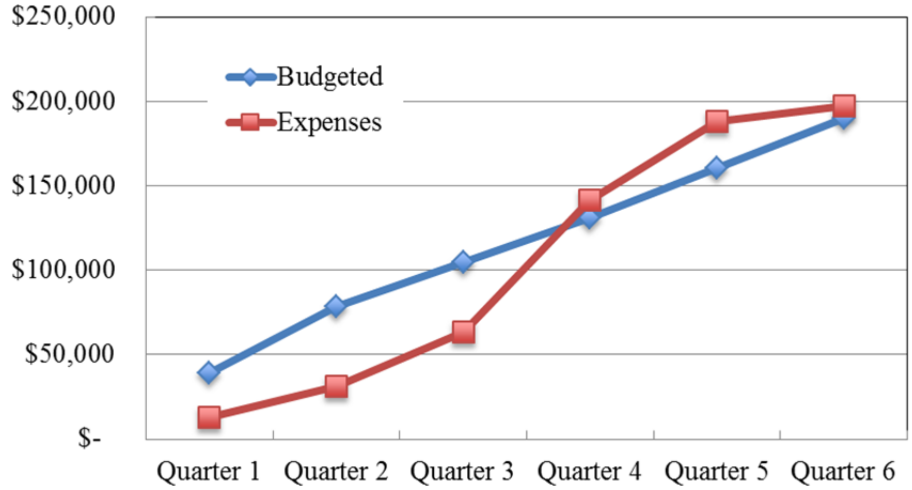

Figure 8 Comparison of OST-R Budget and Expenditure Accumulated by Quarter

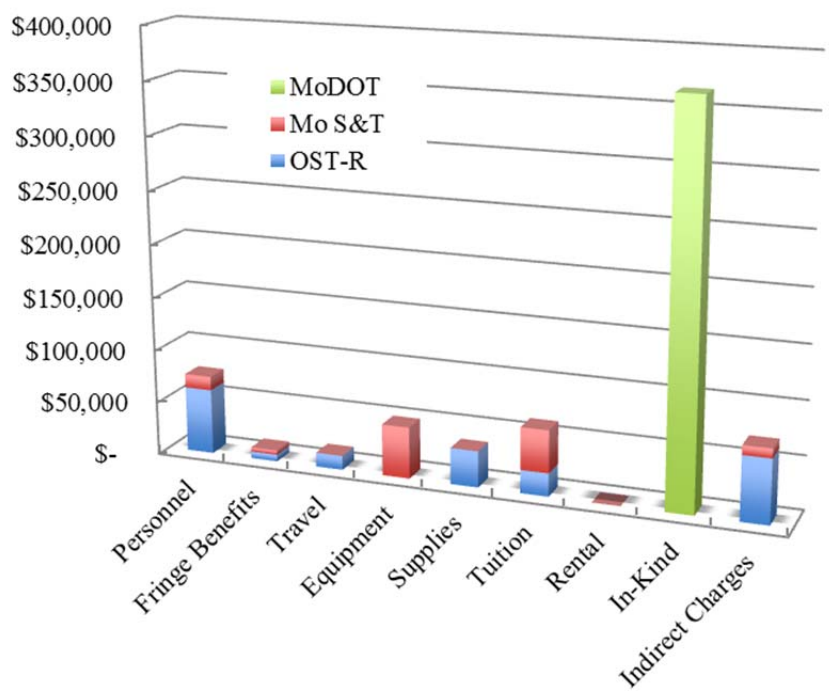

Figure 9 Cummulative Expenditures by Sponsor